International Journal of Nanomedicine

Dovepress
open access to scientific and medical research

Open Access Full Text Article

ORIGINAL RESEARCH

Preparation of Budesonide-Loaded Liposomal Nanoparticles for Pulmonary Delivery and Their Therapeutic Effect in OVA-Induced Asthma in Mice

Xu Zuo[1], Yinuo Gu[1], Xiaoping Guo[1], Wenxue Zheng[1], Haoyu Zheng[1], Yiming An[1], Caina Xu[2,3], Fang Wang[1,3]

[1]Department of Pathogeny Biology, College of Basic Medical Sciences, Jilin University, Changchun, 130021, People's Republic of China; [2]Department of Biochemistry, College of Basic Medical Sciences, Jilin University, Changchun, 130021, People's Republic of China; [3]Key Laboratory of Pathobiology, Ministry of Education, Jilin University, Changchun, 130021, People's Republic of China

Correspondence: Caina Xu; Fang Wang, Email xucaina@jlu.edu.cn; wf@jlu.edu.cn

Purpose: Inhaled corticosteroids, including budesonide (BUD), are widely employed for the treatment of asthma. However, the frequent use of corticosteroids is associated with numerous adverse effects and poses challenges to ongoing drug therapy and patient adherence. Budesonide liposomal nanoparticles (BUD-LNPs) were developed to improve the bioavailability of the drug and thereby improve the effectiveness of asthma treatment.

Methods: BUD-LNPs were prepared via thin-film hydration, and the characterizations, stability, and in vitro release of BUD-LNPs were studied. In vitro cellular uptake was observed by laser-scanning confocal microscope (LSCM) and flow cytometry. And the in vitro anti-inflammatory activity of BUD-LNPs was evaluated by measuring the expression of pro-inflammatory cytokines in activated macrophages. Besides, the accumulation time in the lung of drugs delivered via liposomal carriers and free drugs was compared in vivo. And the in vivo therapeutic efficacy of BUD-LNPs was assessed in OVA-induced asthmatic mice. Finally, in vivo biosafety assessment was performed.

Results: The particle size, PDI, and zeta potential of BUD-LNPs were 127.63±1.33 nm, 0.27±0.02, and 3.33±0.13 mV, respectively. BUD-LNPs exhibited excellent biosafety and anti-inflammatory activity in vitro. Furthermore, compared with the free drugs, the utilization of liposomal nano-vehicles for drugs delivery could effectively extend the duration of drugs accumulation in the pulmonary system. Additionally, treatment with BUD-LNPs alleviated airway hyperresponsiveness, reduced airway mucus secretion, and mitigated pulmonary inflammation in OVA-induced asthmatic mice. And the BUD-LNPs demonstrated superior therapeutic efficacy compared to free BUD.

Conclusion: BUD-LNPs was successfully prepared with excellent stability and sustained release for 24 h in vitro. The data of anti-inflammatory activity, asthma therapeutic effects and safety studies indicated that drug delivery mediated by liposomal nano-vehicles was a feasible and desirable strategy for medical strategy and showed great promise in the clinical therapy of asthma.

Keywords: liposomal nanoparticles, asthma, budesonide, pulmonary delivery, nano-vehicles

Introduction

Asthma is a widely prevalent chronic and heterogeneous ailment affecting individuals of all ages, characterized by the presence of airway hyperresponsiveness, mucus hypersecretion, and chronic inflammation.[1] This condition is often accompanied by distressing symptoms including dyspnea, wheezing, coughing, and chest tightness, with severe cases potentially posing life-threatening risks.[2] The incidence and progression of asthma are influenced by a multitude of factors, including genetic predisposition and environmental conditions. Consequently, there has been a steady rise in the prevalence of asthma, with an estimated global population of approximately 400 million individuals affected by the

Received: 16 October 2023
Accepted: 15 January 2024
Published: 21 January 2024

condition by the year 2025.[3] Despite inhaled corticosteroids are the mainstay of asthma treatment, the current short-acting formulations require frequent administration.[4,5] The endeavor to diminish dosing frequency by augmenting the dosage would result in an initial escalation in drug concentration succeeded by a swift decline, thereby presenting obstacles to both sustained pharmacotherapy and patient compliance.[6] Hence, there is a pressing need for novel therapeutic interventions to effectively manage symptoms and exacerbations in individuals suffering from asthma.

Budesonide (BUD), a glucocorticoid exhibiting potent anti-inflammatory properties and minimal systemic impact, holds promise as a viable pharmaceutical option for managing asthma, allergic rhinitis, and esophagitis.[7,8] Nevertheless, the practical insolubility of BUD in water poses certain constraints on its inhalation-based administration, including the presence of a protective mucosal layer, sustained mucociliary clearance, and limited residence time of the formulation within the nasal cavity or airways.[9] Nanotechnology offered a compelling strategy for enhancing the solubility of drugs with low water solubility by adjusting their size to the nanoscale, thereby substantially augmenting the bioavailability of such drugs.[10,11] Moreover, nanotechnology holds the potential to enhance the efficiency of inhaled drug administration by enabling control over particle size, drug release kinetics, as well as possessing properties that promote mucoadhesion, mucus penetration, and permeation enhancement.[12]

Liposomes are tiny spherical structures composed of one or more amphiphilic phospholipids. They have received extensive attention in pulmonary drug delivery systems due to their advantages, such as biocompatibility, biodegradability, non-toxicity, and non-immunogenicity.[13,14] Compared to other delivery systems, liposomes offer the advantage of encapsulating both hydrophilic and hydrophobic substances. Hydrophilic substances are enclosed within the core of the vesicles, while hydrophobic active substances are integrated into the lipid bilayer.[15] This property not only enhances the bioavailability of various types of drugs, protecting them from premature degradation, but also ensures their controlled delivery.[16] Studies have shown that drugs inhaled via liposomes stayed in the lungs for a longer period of time, which could improve the therapeutic effect of lung tissue and minimize systemic exposure.[17,18] Notably, inhalable liposome suspensions have been approved by the US Food and Drug Administration for clinical use, suggesting that liposomes are the promising carriers.[17]

In this study, we utilized 1,2-dioleoyl-3-trimethylammonium-propane (DOTAP), 1,2-dioleoyl-sn-glycero-3-phosphoethanolamine (DOPE), cholesterol (CHOL), and 1,2-distearoyl-sn-glycero-3-phosphoethanolamine-N- [methoxy (polyethylene glycol)-2000] (DSPE-PEG2000) to prepare BUD-LNPs using the thin film hydration method (Figure 1). We investigated various characteristics of BUD-LNPs, including particle size, zeta-potential, dispersibility, encapsulation efficiency, drug loading efficiency, and in vitro release behavior. Moreover, we conducted in vitro assessments of the biocompatibility of BUD-LNPs and compared the anti-inflammatory abilities of BUD and BUD-LNPs. Additionally, we compared the lung retention time of BUD and BUD-LNPs in mice and evaluated the therapeutic effects of BUD-LNPs using an in vivo mouse asthma model. With satisfactory biocompatibility and therapeutic potential in mind, this study provided novel insights into the design and fabrication of drug delivery systems for future asthma treatment.

Materials and Methods

Materials and Agents

DOTAP (AVT, China, 132172-61-3), DOPE (Macklin, China, 4004-05-1), CHOL (Macklin, China, 57-88-5), DSPE-PEG2000 (Macklin, China, 147867-65-0), rhodamine B (Macklin, China, 81-88-9), budesonide (Aladdin, China, 5137229-3), chloroform and methanol (Beijing Chemical Factory, China), OVA (Sigma-Aldrich, USA, 9006-59-1), $Al(OH)_3$ (Sigma-Aldrich, USA, 77161), Hoechst 33342 (Sigma-Aldrich, USA, 1853314), Cy5-NHS (Meilun Biotechnology, China, 146368-14-1), cell counting Kit-8 (Dojindo, Japan, CK04), mouse IL-4 ELISA kits (Liankebio, China, EK204), mouse IL-5 ELISA kits (Liankebio, China, EK205), mouse IL-13 ELISA kits (Liankebio, China, EK213), AST assay kits (Nanjing Jiancheng, China, C010-2-1), ALT assay kits (Nanjing Jiancheng, China, C009-2-1), AKP assay kits (Nanjing Jiancheng, China, A059-2-2), BUN assay kits (Nanjing Jiancheng, China, C013-2-1), CRE assay kits (Nanjing Jiancheng, China, C011-2-1), UA assay kits (Nanjing Jiancheng, China, C012-2-1).

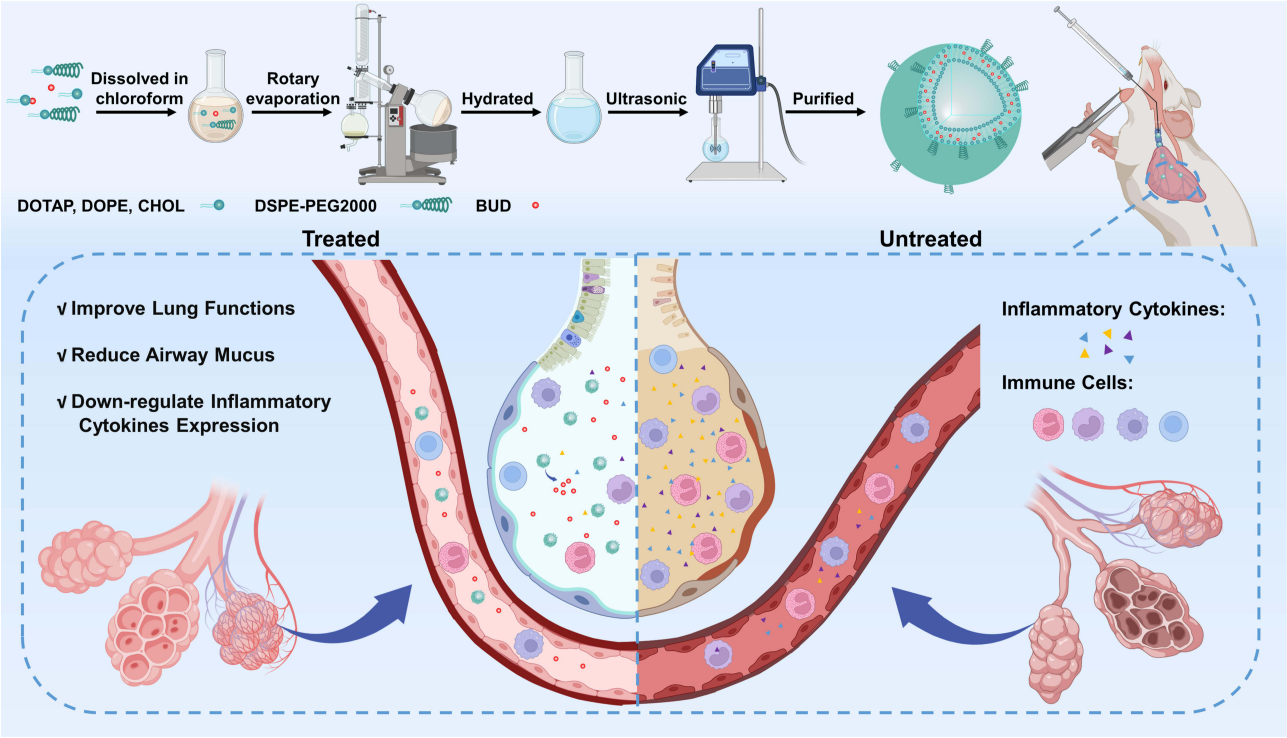

Figure 1 Schematic diagram of BUD-LNPs synthesis and their therapeutic effect in asthmatic mice by pulmonary drug delivery (Created with BioRender.com).

Cell Culture

RAW264.7 cells and the corresponding complete medium were obtained from Zhong Qiao Xin Zhou Biotechnology Co., Ltd. (Shanghai, China). Human lung adenocarcinoma epithelial (A549) cells were purchased from the Chinese Academy of Sciences Cell Bank (Shanghai, China). A549 cells were cultured in Ham's F-12 K medium supplemented with 10% fetal bovine serum (FBS) for optimal growth and maintenance. The cells were cultured in a humidified cell incubator machine at 37 °C and 5% CO_2.

Preparation of Liposomal Nanoparticles

BUD-LNPs were prepared using the thin-film hydration method.[19] To explored the entrapment efficiency (EE) and drug loading (DL) of nanoparticles synthesized by BUD at different concentrations to find the most appropriate ratio. We synthesized three different proportions of nanoparticles: BUD-LNPs-1 (DOTAP: DOPE: CHOL: DSPE-PEG2000: BUD = 8.4 mg: 22.3 mg: 7.7 mg: 19.6 mg: 2 mg); BUD-LNPs-2 (DOTAP: DOPE: CHOL: DSPE-PEG2000: BUD = 8.4 mg: 22.3 mg: 7.7 mg: 19.6 mg: 4 mg); and BUD-LNPs-3 (DOTAP: DOPE: CHOL: DSPE-PEG2000: BUD = 8.4 mg: 22.3 mg: 7.7 mg: 19.6 mg: 8 mg). Briefly, DOTAP, DOPE, CHOL, DSPE-PEG2000 and BUD were dissolved in chloroform The organic phase was evaporated using a rotary evaporator to form a lipid film. The lipid film was then hydrated with 8 mL of PBS at 37°C for 2 h. Subsequently, the liposome solution was sonicated at 100 W for 10 min in an ice-water bath, and the BUD-LNPs were centrifuged three times at 1000 rpm and passed through the 0.45 μm filter three times to remove free BUD. In addition, the preparation of liposomal nanoparticles (LNPs) without BUD served as a control.

Rhodamine-B liposomal nanoparticles (Rhodamine B-LNPs) were also prepared as follows. DOTAP, DOPE, CHOL, DSPE-PEG2000 were dissolved in chloroform, and thin films were formed using rotary evaporation. The lipid film was rehydrated with 8 mL of Rhodamine B-containing PBS for a period of 2 h. and the solution was sonicated at 100 W for 10 min in an ice-water bath. Subsequently, Rhodamine B-LNPs were dialyzed against PBS (0.01 M), to remove free Rhodamine B. Similarly, in the preparation of Cy5-liposomal nanoparticles (Cy5-LNPs), Rhodamine B was replaced with Cy5, while the remaining steps remained the same as described above.

Characterization of Liposomal Nanoparticles

The liposomal nanoparticles formulations were diluted to a concentration of 0.5 mg/mL, and the particle size, polydispersity index (PDI), and zeta-potential were determined using Nano Sizer and Zeta-potential analyzer (Malvern Instruments, UK). The liposomal nanoparticles samples were diluted and dropped on the surface of the copper grid, stained with phosphotungstic acid (3%, w/v), and then observed under a TEM (JEM-1200 EX, Japan). To determine the DL and EE of BUD, free BUD was isolated by centrifugation at 1000 rpm for 10 min. And the BUD-LNPs were sonicated with methanol for 5 min in an ice bath to break up their lipid membranes. The amount of BUD in BUD-LNPs was determined by high-performance liquid chromatography (HPLC, Shimadzu, Japan) at 240 nm. The DL and EE of BUD were calculated using the following formulas (Equations 1 and 2):

$$DL(\%)=(W_{BUD\ in\ LNPs}/W_{LNPs})\ \times\ 100\% \tag{1}$$

$$EE(\%)=(W_{BUD\ in\ LNPs}/W_{total\ BUD})\ \times\ 100\% \tag{2}$$

where $W_{BUD\ in\ LNPs}$ was the weight of BUD after centrifugation, W_{LNPs} was the weight of LNPs (BUD + liposomes), and $W_{total\ BUD}$ was the weight of drugs initially fed.

In vitro Release Rate of BUD

The in vitro release rate of BUD in BUD-LNPs was analyzed using a dialysis method. The dialysis bag containing a 2 mL BUD-LNPs solution was immersed in 200 mL of PBS (pH 7.4) and subjected to gentle stirring using a magnetic stirrer. At predetermined time points, 1 mL of the solution was withdrawn and replaced with 1 mL of PBS. The amount of BUD released into the collected liquid was quantified using HPLC.

Stability of BUD-LNPs

To explore the stability of BUD-LNPs, they were dispersed in PBS containing 10% FBS and incubated at 37°C. Measure the size distribution and zeta-potential of BUD-LNPs using DLS at 0 h, 2 h, 4 h, 6 h, 8 h, 12 h, 24 h, 36 h, 48 h, and 72 h, respectively.[20]

In vitro Cytotoxicity

CCK-8 assay was used to evaluate the cytotoxicity of BUD-LNPs and LNPs to RAW264.7 cells and A549 cells. Cells were seeded in 96-well plates at a density of 8.0×10^3 per well. After the cells adhered to the wall, they were exposed to BUD-LNPs and LNPs at concentrations of 300, 200, 100, 50 μg/mL and BUD at concentrations of 5.7 μg/mL, respectively. After the cells were incubated for 24 h, the culture medium containing 10 μL of CCK-8 was further incubated at 37 °C for 1 h. Optical density (OD) was measured at 450 nm by a microplate reader. Untreated cells were used as controls. All measurements were performed in triplicate. Cell viability was determined by calculating the optical density value using the following formula (Equation 3):

$$\text{Cell viability}(\%) = (\text{OD of test} - \text{OD of blank})/(\text{OD of control} - \text{OD of blank})\ \times\ 100\% \tag{3}$$

Observation of Cellular Internalization Profiles of Nanoparticles by LSCM

RAW264.7 cells were seeded in 24-well plates at a density of 1×10^5 cells/well and incubated overnight at 37 °C and 5% CO_2. To investigate the cellular internalization of Rhodamine-LNPs at different concentrations, we incubated cells with Rhodamine-LNPs at 10, 50, and 100 μg/mL for 12 h. Then, wash the cells three times with 500 μL PBS to remove cell debris or Rhodamine-LNPs that were not taken up by the cells. Then Hoechst 33342 (10 μg/mL) was added as a nuclear dye, and the incubation time was 20 min. Cellular uptake was observed under a LSCM (FV3000, Olympus). And using similar methods, RAW264.7 cells were treated with Rhodamine-LNPs (100 μg/mL) for 1 h, 6 h, and 12 h, respectively to observe the internalization situation at different times.

Flow Cytometric Analysis of Cellular Uptake of Nanoparticles

RAW264.7 cells 2×10^5 cells/well were cultured in 12-well plates for 12 h. Then cells were incubated with 100 μg/mL Cy5-LNPs. Then, wash the cells three times with 500 μL PBS to remove cell debris or Cy5-LNPs that were not taken up by the cells. At predetermined time points (1, 6 and 12 h), cells were harvested for flow cytometric analysis (Accuri C6, BD, USA).

LPS Stimulation and BUD-LNPs Treatment in RAW264.7 Cells

The LPS stimulation treatment of RAW264.7 cells and the corresponding complete medium were purchased from Zhong Qiao Xin Zhou Biotechnology Co., Ltd. Cells were cultured in a humidified cell culture machine at 5% CO_2 and 37 °C. The experiment was divided into five groups: control group (PBS group), cells were treated with PBS; LPS group (LPS), cells were treated with LPS (1 μg/mL) for 6 h; LNPs group (LNPs), cells were treated with LNPs (100 μg/mL) cells treated for 24 h after LPS treatment. BUD group (BUD), cells treated with BUD (5.7 μg/mL) for 24 h after LPS treatment. BUD-LNPs group (BUD-LNPs), cells treated with BUD-LNPs (100 μg/mL) for 24 h after LPS treatment.

In vivo Distribution of Cy5-LNPs

All animal experiments were performed in accordance with the guidelines approved by the Animal Care and Use Review Committee of Jilin University. Female Balb/c mice aged 6–8 weeks and weighing 18–20 g were randomly divided into two groups: free Cy5 group and Cy5-LNPs group. Firstly, mice were anesthetized with isoflurane, then the pulmonary drug delivery device was used to give 30 μL Cy5-LNPs solution to the trachea of Cy5-LNPs group mice, and free Cy5 group was given the same amount of free Cy5 solution as Cy5-LNPs group. In order to observe the accumulation of drugs in the lungs at different time points, mice were anesthetized and euthanized at different time points (1 h, 6 h, 12 h, and 24 h), and the major organs (liver, heart, spleen, lungs, and kidneys) were removed for fluorescence imaging (IVIS Spectrum). Three mice were sampled at each time point and used for the statistical analysis of fluorescence intensity.

Animals

SPF female Balb/c mice aged 6–8 weeks and weighing 18–20 g were purchased from Yisi Laboratory Animal Technology Co., Ltd. (Changchun, China, 01021702619076288). The experimental manipulation of the mice was undertaken in accordance with the National Institute of Health Guide for the Care and Use of Laboratory Animals. The mouse experiments were approved by the ethics committee of the College of Basic Medical Sciences of Jilin University with the number 2023–446. And the license number of the mouse animal center is SYXK(Ji)2023–0010.

Murine Asthma Model

Female Balb/c mice aged 6–8 weeks and weighing 18–20 g were randomly divided into control group (PBS), OVA group (model group), LNPs group, BUD group and BUD-LNPs group, a total of 5 groups (n = 6). On days 0, 7, and 14, each mouse in the OVA, LNPs, BUD, and BUD-LNPs groups was sensitized by intraperitoneal injection of PBS containing 50 μg OVA and 25 μL $Al(OH)_3$. At the same time, the control group was injected with the same amount of PBS. On days 21–23, each mouse in the OVA group, LNPs group, BUD group, and BUD-LNPs group was challenged with 3% OVA solution for 45 min per day. Mice in the control group were sham-sensitized and challenged with an equal volume of PBS. On days 21–23, mice in each group were anesthetized with isoflurane. The BUD-LNPs group administered 30 μL of BUD-LNPs solution to the mouse trachea using the pulmonary drug delivery device (the amount containing BUD was 0.5 mg/kg). The same amount of BUD solution was given to the BUD-LNPs group, and 30 μL PBS was given intratracheally by the pulmonary drug delivery device in the control group and OVA group. On day 24, all mice were anesthetized and euthanized for further experiments.

Bronchial Alveolar Lavage Fluid (BALF) Collection

To obtain BALF, the trachea of the euthanized mouse was exposed and connected to a syringe, and the lungs were repeatedly lavaged 3 times with 1 mL of sterile saline to collect the fluid. The resulting liquid was centrifuged (400×g, 5 min, 4°C), and the supernatant was taken to test the IL-4, IL-5, and IL-13 ELISA kits.

Enzyme-Linked Immunosorbent Assays (ELISAs)

ELISA kits were utilized to quantify the expression levels of cytokines IL-4, IL-5, and IL-13 in lung tissue. The procedures were carried out in accordance with the manufacturer's recommendations and were repeated three times.

Lung Function Measurement

The DSI Buxco FinePoint RC system (DSI Buxco, USA) as described in previous studies, was utilized for invasive lung function testing.[21,22] Once the mice were deeply anesthetized, they were positioned and intubated through the trachea to ensure proper ventilation. The experimental setup involved connecting the animal chamber to a spirometer, pneumatic sensor, and pressure sensor. Once the mice achieved stable breathing patterns without any interference from the equipment, the spirometer automatically measured and evaluated various lung function parameters.

Hematoxylin-Eosin (H&E) Staining

After harvesting BALF, lungs of mice were excised, rinsed with PBS, and fixed in 4% paraformaldehyde (PFA). Subsequently, lungs were embedded in paraffin and cut into 3–4 μm thick sections. And H&E staining was performed on paraffin sections to examine histopathological features.

Alcian Blue Periodic Acid Schiff (AB-PAS) Staining

After euthanasia, the mice were tracheotomized and intubated. The airway was treated the mixture of vehicle and saline (0.8 mL) by the syringe. After tightening the sutures and closing the trachea with a knot, the lungs were removed and immersed in 4% paraformaldehyde (PFA). Afterwards, the lungs were frozen and embedded in medium at an optimal cutting temperature and sectioned. The sections were placed on glass slides and stained with AB-PAS reagent. Finally, observed with the Olympus BX53 microscope, taken pictures and saved the data for subsequent analysis.

In vivo Toxicity Test

Female Balb/c mice, aged 6–8 weeks and weighing 18–20 g, were randomly divided into four groups: the PBS group, BUD group, LNPs group, and BUD-LNPs group, each comprising three mice. The BUD group, LNPs group, and BUD-LNPs group were administered 30 μL of BUD (5.7 μg/mL), LNPs (100 μg/mL), and BUD-LNPs (100 μg/mL) into the airway, respectively, using a pulmonary drug delivery device. In the PBS group, 30 μL of PBS was administered into the airway in the same manner. On day 4, peripheral blood from mice in each group was collected in Microtainer® EDTA-coated tubes and serum separation tubes. Approximately 600 mL of peripheral blood was then centrifuged for 20 min to obtain the supernatant. Aspartate aminotransferase (AST), alanine aminotransferase (ALT), alkaline phosphatase (AKP), urea nitrogen (BUN), uric acid (UA), creatinine (CRE) levels were determined using the assay kits (Nanjing Jiancheng Bioengineering Institute), respectively. And the hearts, livers, spleens, lungs, and kidneys of mice in each group were washed with PBS and fixed in 4% paraformaldehyde, embedded in paraffin and sectioned. Paraffin sections were then stained with hematoxylin and eosin to assess histopathological features.

Statistical Analysis

The results were shown as mean ± standard deviation. Data sets were processed and plotted in GraphPad Prism 9. Comparisons between groups were performed by one-way analysis of variance (ANOVA). Values of $P<0.05$ means the difference was statistically significant.

Results and Discussion

Physicochemical Characterization of BUD-LNPs

LNPs and BUD-LNPs were prepared using the thin-film hydration method. We explored the EE and DL of nanoparticles synthesized by BUD at different concentrations to find the most appropriate ratio. Among them, the EE and the DL of BUD-LNPs-1 were 81.03% and 2.71%; the EE and DL of BUD-LNPs-2 were 78.63% and 5.75%; and the EE and DL of BUD-LNPs-3 were 43.70% and 5.53% (Table 1). Based on the results, we selected BUD-LNPs-2 as the synthesis

Table 1 Diameter, Zeta-Potential, EE and DL of LNPs and BUD-LNPs-1, BUD-LNPs-2 and BUD-LNPs-3. (n = 3)

Nanoparticles	Diameter (nm)	Zeta-Potential (mV)	EE (%)	DL (%)
LNPs	125.37 ± 2.94	6.00 ± 0.07	–	–
BUD-LNPs-1	126.61 ± 1.74	3.41 ± 0.21	81.03 ± 0.24	2.71 ± 0.47
BUD-LNPs-2	127.63 ± 1.33	3.33 ± 0.13	78.63 ± 0.38	5.75 ± 0.18
BUD-LNPs-3	125.58 ± 1.96	3.03 ± 0.44	43.70 ± 0.47	5.53 ± 0.27

solution for the following experiments. Hereinafter referred to as BUD-LNPs. The particles size measured by the Nano Sizer and Zeta-potential analyzer of the different samples were presented in Table 1. The particle size of LNPs were determined to be 125.37±2.94 nm (Figure 2a), while BUD-LNPs had a particle size of approximately 127.63±1.33 nm (Figure 2b). Notably, the inflammatory immune response caused by asthma results in airway obstruction, while excessive mucous production further restricts airflow.[23,24] Specifically, mucin fibers create dense macromolecular networks through chemical crosslinking or physical entanglement, thereby impeding the diffusion of particles in space, particularly when the nanoparticle diameter reaches or exceeds the mesh size of the mucus gel. Numerous studies have indicated that the average pore size of human airway mucus is estimated to be approximately 200 nm.[25,26] Hence, the size of our prepared nanoparticles must meet certain criteria to traverse the mucus layer effectively. Besides, the presence of PEG in the synthetic constituents can aid in facilitating the passage of nanoparticles through the mucus layer.[25] Consequently, BUD-LNPs demonstrated promising potential for efficient delivery to the alveoli following pulmonary inhalation. Additionally, the morphology of the BUD-LNPs was characterized using TEM (Figure 2c). And the zeta-potential measured by the Nano Sizer and Zeta-potential analyzer of LNPs were determined to be 6.00±0.07 mV, while BUD-LNPs had a zeta-potential of 3.33±0.13 mV (Figure 2d), which enhanced their interaction with the negatively charged mucus network and facilitated their penetration and retention in the lungs.[27]

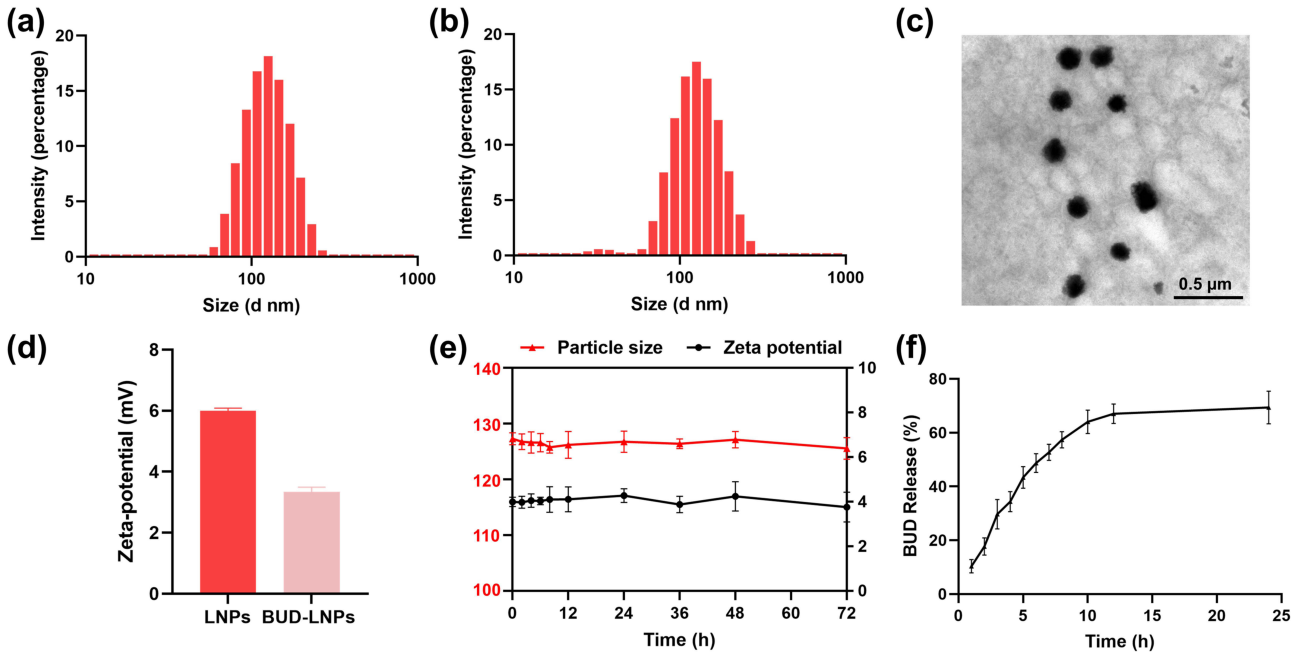

Figure 2 Characterization of BUD-LNPs. (**a**) Particle size distribution of LNPs measured by Nano Sizer and Zeta-potential analyzer. (**b**) Particle size distribution of BUD-LNPs measured by Nano Sizer and Zeta-potential analyzer. (**c**) TEM images of BUD-LNPs. Scale bar: 0.5 μm. (**d**) Zeta potentials of the different samples measured by Nano Sizer and Zeta-potential analyzer (n = 3). (**e**) The stability of BUD-LNPs formulations measured by Nano Sizer and Zeta-potential analyzer. (n = 3). (**f**) Cumulative release of BUD from BUD-LNPs formulations at pH 7.4 (n = 3).

Furthermore, the stability of BUD-LNPs were dispersed in PBS containing 10% fetal bovine serum (FBS) and incubated at 37 °C. The particle size distribution and zeta-potential of BUD-LNPs were measured at 0, 2, 4, 6, 8, 12, and 24 h using the Nano Sizer and Zeta-potential analyzer. As shown in Figure 2e, the particle size and zeta-potential of BUD-LNPs remained stable within 72 h in PBS (10% FBS) without significant changes, which suggested that BUD-LNPs were quite stable in the circulation. Moreover, to investigate the in vitro release efficiency of BUD-LNPs, HPLC was used to measure BUD release in PBS. As depicted in Figure 2f, BUD-LNPs exhibited a slowly release rate within 24 h, which suggested that the drug would be sustained in the lung for future in vivo pulmonary administration. It also showed that they may increase the residence time of the drug in the lungs and reduce the side effects of the drug on other organs.

Cytotoxicity and Cellular Uptake

Since the potential toxicity of the pulmonary drug delivery is of vital importance in clinical application, the cytocompatibility of LNPs, BUD-LNPs and BUD was assessed by a CCK-8 assay by culturing them with RAW264.7 cells and A549 cells. Macrophages are employed in toxicity studies because they are the body's first line of defense and the first cells to recognize foreign substances such as drug carriers.[28] A549 cells were chosen because they are a mouse lung epithelial cell line commonly used to study the toxicity of nanoparticles.[29,30] Figure 3a showed the cell viability of RAW264.7 cells after 24 h treatment with LNPs and BUD-LNPs. Even at a concentration of 300 μg/mL, both LNPs and BUD-LNPs induced negligible changes in cell viability, indicating their low toxicity and excellent biocompatibility. Additionally, Figure 3b showed the cell viability of A549 cells after 24 h treatment with LNPs and BUD-LNPs showed similar results to RAW264.7 cells. Moreover, in the following anti-inflammatory experiments, the concentration of BUD calculated based on the encapsulation efficiency was 5.7 μg/mL, which also showed no obvious damage to the cells. These observations suggested that LNPs and BUD-LNPs showed a high percentage of viable cells, which further supported the acceptable biocompatibility.

Furthermore, Rhodamine B-LNPs using rhodamine-B instead of BUD was prepared as red fluorescence for visualization. Cellular uptake of Rhodamine B-LNPs was investigated by the LSCM using RAW264.7 cells.[19] LSCM observations showed dose-responsive internalization of Rhodamine B-LNPs by RAW264.7 cells (Figure S1). And the fluorescence images of Figure 3c showed that Rhodamine B-LNPs had a weak affinity for incubation with RAW264.7 cells. Furthermore, it could be seen that the incubation of Rhodamine B-LNPs with RAW264.7 cells had a stronger affinity at 12 hours. These observations indicated that Rhodamine B-LNPs showed a strong affinity with RAW264.7 cells, and the affinity increased with time. And the flow cytometric analysis of cellular uptake of Cy5-LNPs also revealed similar results (Figure S2). These might be due to the fact that PEGylated liposomal nanoparticles can maintain higher affinity intensity for a longer time in vitro.

Anti-Inflammatory Activities of BUD-LNPs

To mimic the inflammatory microenvironment, we utilized RAW264.7 cells to activate macrophages by LPS treatment.[31,32] As shown in Figure 4a, LPS stimulation resulted in significant upregulation of IL-6 ($P < 0.001$). BUD (5.7 μg/mL) and BUD-LNPs (100 μg/mL) both exhibited strong inhibitory effects on the upregulation of IL-6 ($P < 0.01$). While LNPs exhibited no inhibitory effects on the upregulation of IL-6. As shown in Figure 4b, the inhibitory effects of them on TNF-α showed similar results to those of IL-6. LPS stimulation resulted in significant upregulation of TNF-α ($P < 0.001$). BUD (5.7 μg/mL) and BUD-LNPs (100 μg/mL) both exhibited marked inhibitory effects on the upregulation of TNF-α level. While LNPs exhibited little inhibitory effects on the upregulation of TNF-α level. The above results indicated that BUD-LNPs had excellent anti-inflammatory activity in vitro. Asthma is a chronic respiratory disease characterized by airway inflammation even in mild cases,[33] so anti-inflammatory activity in vitro had great advantage for the treatment of asthma in vivo.

In vivo Lung Accumulation of Cy5-LNPs

As an excellent drug delivery carrier, liposomal nanoparticles exhibited outstanding properties, such as protecting encapsulated substances from physiological degradation, controlling the release of drug molecules, prolonging the

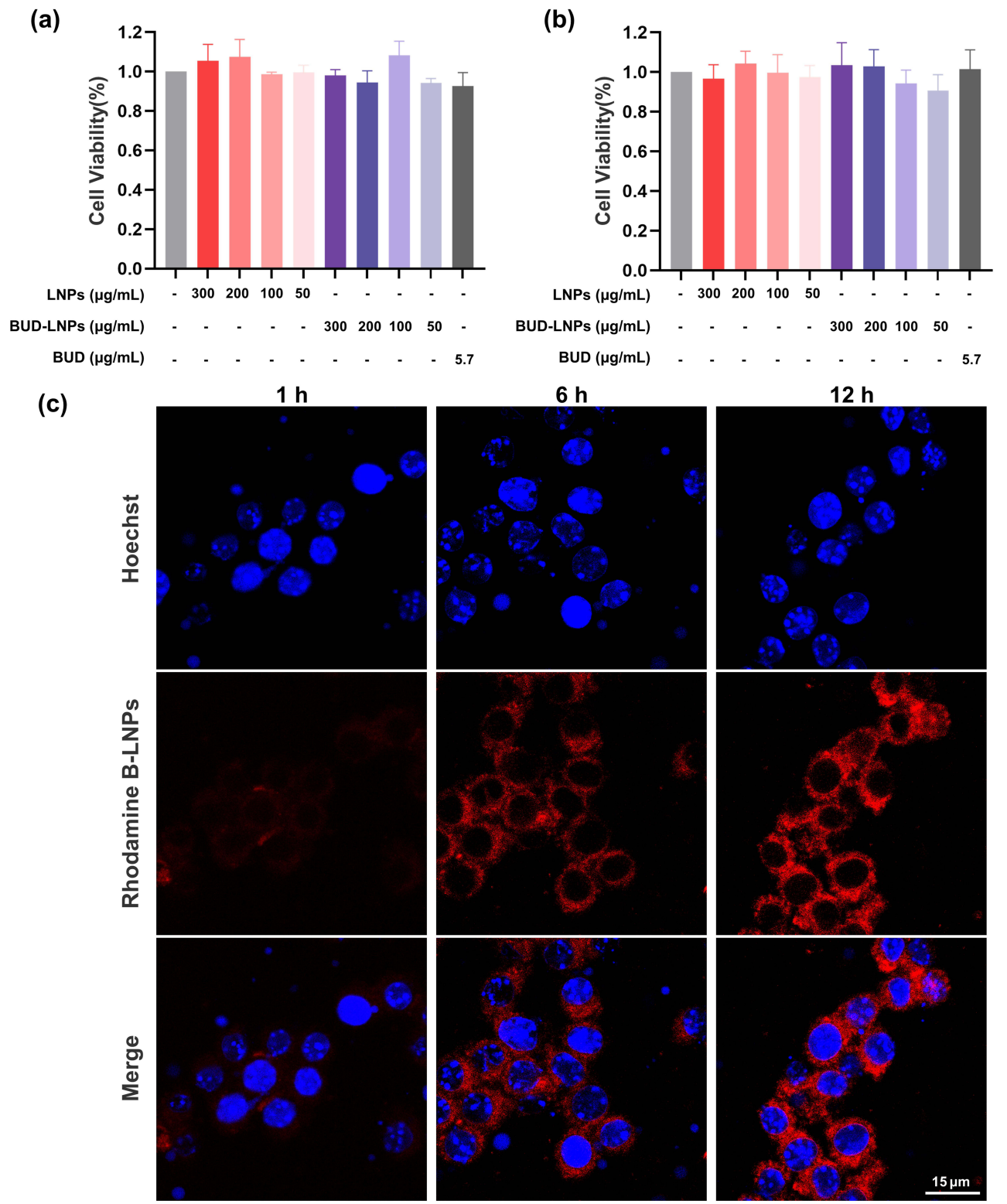

Figure 3 The toxicity of BUD-LNPs on A549 cells and RAW264.7 cells, as well as the uptake by RAW264.7 cells. (**a**) RAW264.7 cells viability after the treatment with different samples (n = 3). (**b**) A549 cells viability after the treatment with different samples (n = 3). (**c**) Cellular uptake of Rhodamine B-LNPs on RAW264.7 cells after 1 h, 6 h, and 12 h of incubation, measured by LSCM. Scale bar: 15 μm.

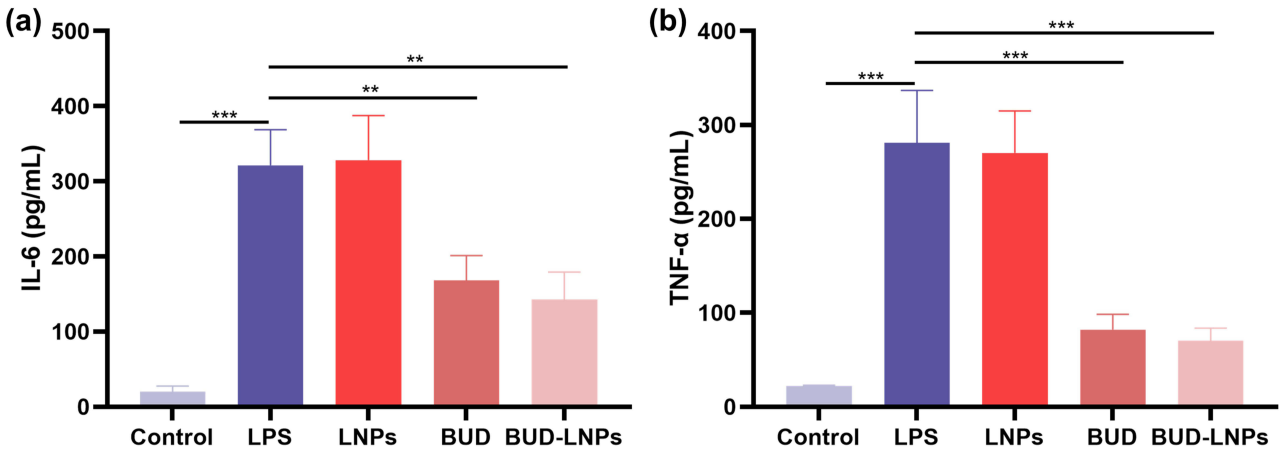

Figure 4 Anti-inflammatory effect of different samples against RAW264.7 cells. (**a**) The effects of different samples on the level of IL-6. (**b**) The effects of different samples on the level of TNF-α. Data were presented as mean ± S.D., (n = 3) $^{**}P < 0.01$; $^{***}P < 0.001$.

administration time, etc.[13,15,34] To investigate the accumulation of free Cy5 and Cy5-LNPs in the lung tissues, Cy5-LNPs were prepared and delivered into the trachea using the pulmonary drug delivery device. In vivo imaging was used to observe the accumulation of free Cy5 and Cy5-LNPs in lung tissue at different time points. The results of the lung images showed that a homogeneous fluorescence distribution after administration via pulmonary drug delivery device, suggesting that the Cy5-LNPs and free Cy5 could be effectively and uniformly distributed throughout the lungs. Furthermore, after 24 h of administration, the Cy5-LNPs group still showed strong fluorescence intensity, and it could be seen that there was a significant difference in the accumulate time between free Cy5 and Cy5-LNPs (Figures 5 and S3). The above results suggested that the utilization of liposomal nanoparticles for drug delivery can effectively extend the duration of drug presence in the pulmonary system. Consequently, this may result in a decreased frequency of inhalation required by patients, thereby enhancing patient adherence and rendering it a promising drug delivery material for the advancement of asthma medication.

Asthma Therapeutic Effect of BUD-LNPs

The animal model of asthma yields valuable insights into the characteristics of asthma pathogenesis and treatment.[35] Next, we assessed the therapeutic efficacy of BUD-LNPs in the mouse model of asthma. Asthmatic mice were induced by sensitizing them with OVA/alum on days 0, 7, and 14, followed by OVA aerosol challenges on days 21 to 23. Subsequently, on days 21 to 23, the pulmonary drug delivery device was used to directly intratracheally spray BUD, LNPs, and BUD-LNPs into the airways of mice (Figure 6a).

Lung function testing plays a crucial role in clinically evaluating the extent and reversibility of airflow limitation in individuals diagnosed with asthma.[36] As shown in Figure 6b and c, compared with the PBS group, the airway resistance of the mice in the OVA group was significantly increased ($P<0.001$), Elevated airway resistance made the breathing more difficult, showing rapid breathing, increased breathing rate, wheezing, and coughing.[37] After the intervention of BUD and BUD-LNPs, the airway resistance of the mice was improved, and there was statistical difference ($P<0.05$). This result meaned that BUD-LNPs had a certain intervention effect on asthma-induced airway obstruction. Besides, after intervention with BUD and BUD-LNPs, the dynamic compliance of mice improved significantly (Figure 6d and e). This indicated that the mice experienced smoother breathing, with a more effective increase in expiratory volume and an increase in respiratory depth during expiration. In conclusion, airway hyperresponsiveness was a clinical feature of asthma that was generally proportional to the underlying severity of the disease.[38] Airway resistance and dynamic compliance were important indicators for evaluating airway hyperresponsiveness. BUD-LNPs significantly improved airway hyperresponsiveness in OVA-induced asthmatic mice, effectively alleviated symptoms, and controlled the development of the disease. And BUD-LNPs group had obvious therapeutic advantage compared with BUD group ($P<0.05$). This may be due to the persistent pulmonary accumulation of BUD delivered by liposomal nano-vehicles.

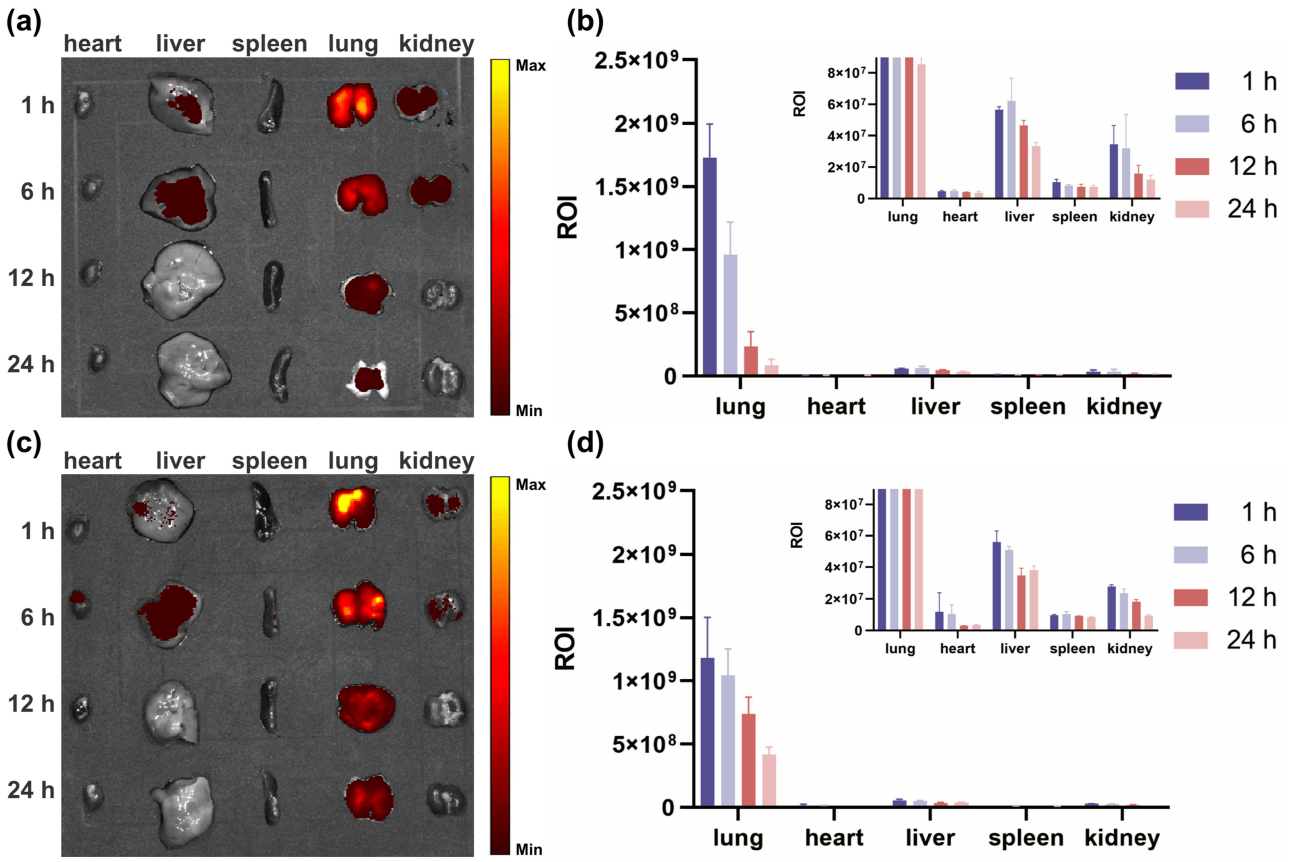

Figure 5 Ex vivo fluorescence images (**a**) and quantitative data (**b**) showed the distribution of Cy5 following intra-airway administration in the heart, liver, spleen, lungs, and kidneys at different time points Data were presented as mean ± S.D., (n = 3). Ex vivo fluorescence images (**c**) and quantitative data (**d**) showed the distribution of Cy5-LNPs following intra-airway administration in the heart, liver, spleen, lungs, and kidneys at different time points Data were presented as mean ± S.D., (n = 3). The insets of (**b** and **d**) represented local magnifications.
Abbreviation: ROI, region of interest.

Airway mucus hypersecretion is one of the pathophysiological features of asthma.[39] Since clinicians identified mucus plugs as a fatal factor in asthmatic patients in the 1880s, his phenomenon has been continuously and rigorously studied.[24] Consequently, whether airway mucus is effectively cleared is critical for evaluating the effect of asthma treatment. The obstruction of mucus in the bronchi and alveoli was visualized with AB-PAS staining (Figure 7a). The results showed that the purple-blue color in the trachea and alveoli was a mixture of neutral and acidic mucus. The level of airway mucus secretion was significantly higher in the OVA group compared with the control group, suggesting significant mucus accumulation in the airways of asthmatic mice. After the intervention of BUD and BUD-LNPs, the mucus secretion was significantly cleared compared with the OVA group, and the LNPs group had no obvious treatment effect. This result indicated that BUD-LNPs had significant mucus-clearing efficacy, and LNPs did not have the function of improving the mucus environment. Furthermore, H&E staining was performed on the lung tissue of mice in each group to investigate the therapeutic effects of BUD-LNPs on lung inflammation and to assess the alveolar structure and infiltration of inflammatory cells in the airways (Figure 7b). In the OVA group, noticeable pathological changes were observed, including bronchial thickening, alveolar septum thickening, alveolar fusion, and inflammatory cell infiltration in all layers of the bronchial wall. And the LNPs group did not show any improvement in these parameters. However, in the BUD and BUD-LNPs groups, improvements in bronchial thickening, restoration of alveolar septa, and a significant reduction in inflammatory cell infiltration were observed. Compared with the free BUD group, the BUD-LNPs group showed a better therapeutic effect. This improvement may be attributed to the prolonged release time and increased the bioavailability of BUD delivered by liposomal nano-vehicles in the body, which enhanced the airway microenvironment for a longer duration and reduced mucus production.

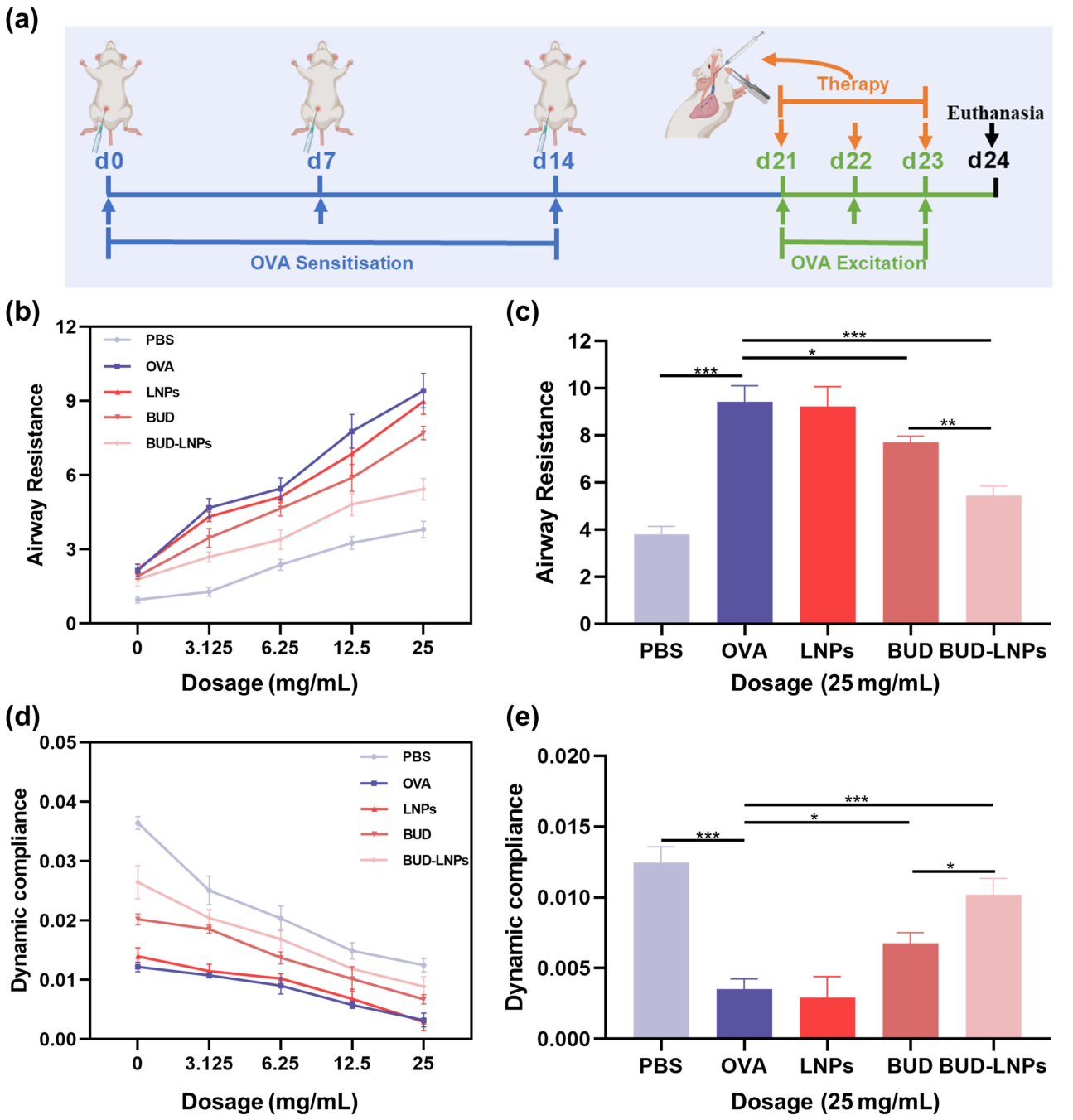

Figure 6 BUD-LNPs improved lung function in OVA-induced asthmatic mice (Created with BioRender.com). (**a**) Schematic diagram of in vivo model establishment and treatment. (**b**) Respiratory system resistance in response to increasing concentrations of methacholine. (**c**) Respiratory system resistance in response to 25 mg/mL methacholine. (**d**) Dynamic compliance in response to increasing concentrations of methacholine. (**e**) Dynamic compliance in response to 25 mg/mL methacholine. Data were presented as mean ± S.D., (n = 6) **P* < 0.05; ***P* < 0.01; ****P* < 0.001.

Cytokines released by Th2 cells, including interleukin IL-4, IL-5, and IL-13, play a crucial role in the progression of asthma.[40] These cytokines are closely associated with bronchial inflammation, smooth muscle spasm, and airway mucus hypersecretion. Furthermore, they contribute to irreversible airway remodeling, excessive fibrosis, and the deposition of collagen, thereby exacerbating the disease process.[41] Therefore, in order to further explore the effect of BUN-LNPs on the expression levels of inflammatory factors in the alveolar lavage fluid of mice in each group of OVA-induced asthma model, we evaluated the lung inflammation by measuring the levels of IL-4, IL-5 and IL-13 inflammatory cytokines (Figure 7c–e).

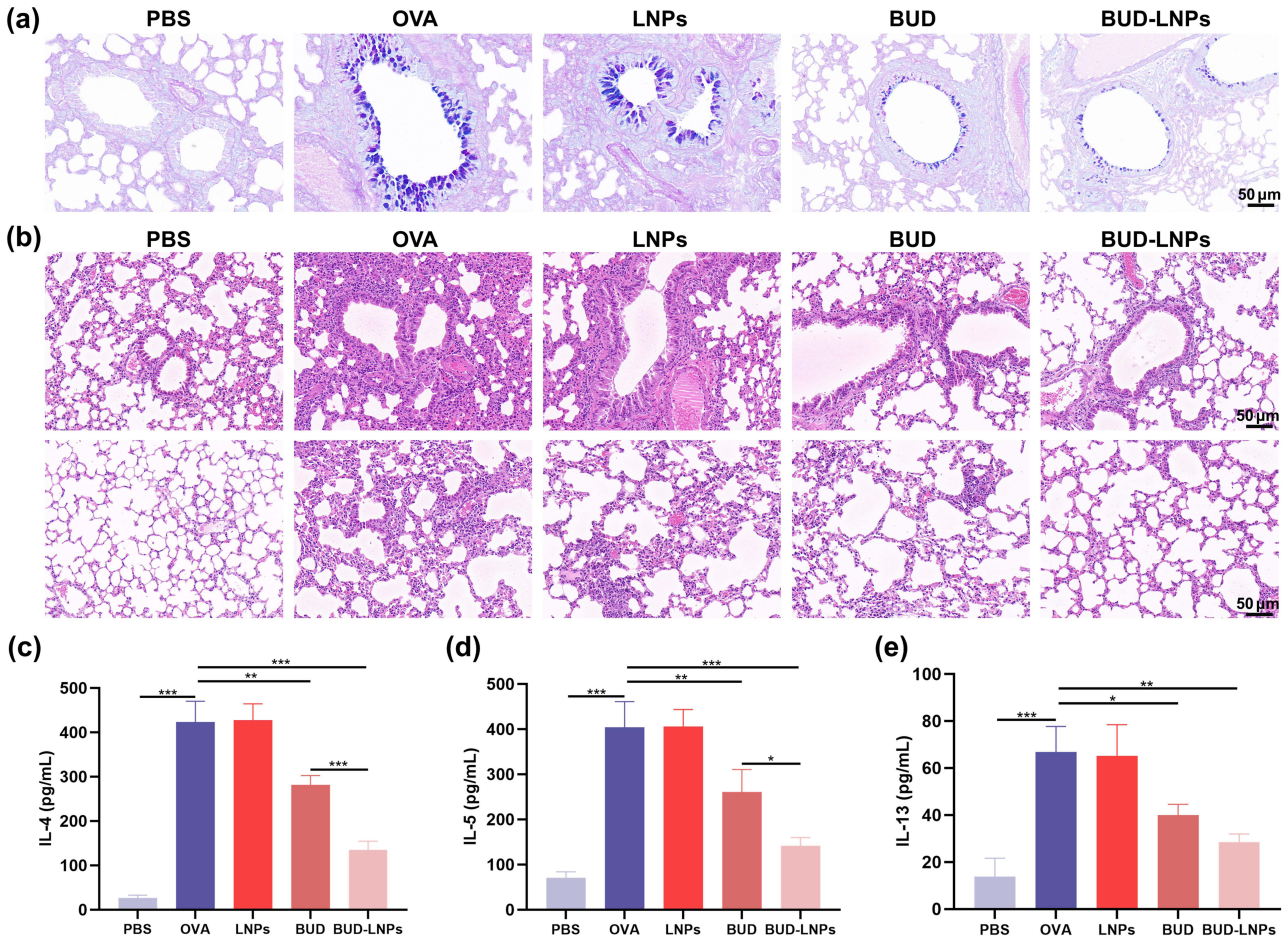

Figure 7 Therapeutic effect of BUD-LNPs on OVA-induced asthma in mice. (**a**) Images of respiratory bronchioles and alveoli stained with AB-PAS after undergoing various treatments. Scale bar: 50 μm. (**b**) H&E staining images of respiratory bronchioles and alveoli after different treatments. Scale bar: 50 μm. The results of ELISA about protein levels of cytokines (**c**) IL-4, (**d**) IL-5, (**e**) IL-13 of supernatant from BALF. Data were presented as mean ± S.D. (n = 6) **P* < 0.05; ***P* < 0.01; ****P* < 0.001.

Compared with the control group, the levels of IL-4, IL-5 and IL-13 in the BALF of mice in the OVA group were significantly increased, indicating that OVA induced increased lung inflammation in the asthmatic model group. After the mice treated with BUD and BUD-LNPs, the expressions of IL-4, IL-5 and IL-13 were significantly reduced. This indicated that airway inflammation was reduced in the BUD group and BUD-LNPs groups. From the above results, BUD-LNPs significantly improved the lung function, alleviated lung inflammation, and cleared airway mucus in OVA-induced asthmatic mice. BUD, as a glucocorticoid, has high anti-inflammatory activity and low systemic effects due to high receptor affinity and airway selectivity.[42] The liposomal nano-vehicles delivered and given directly to the lungs, which improved the bioavailability of budesonide, prolonged the release time of the drug, and maximizes the effect of the drugs. In conclusion, BUD-LNPs have great prospects in the development of new drugs for the treatment of asthma in the future.

In vivo Safety Assessment

After in vivo therapeutic evaluation, the in vivo safety of BUD, LNPs, and BUD-LNPs was assessed through the histopathological observation of heart, liver, spleen, lung and kidney. As shown in Figure 8a, after the healthy mice administration of BUD, LNPs, and BUD-LNPs, the heart, liver, spleen, lung and kidney of them were observed histopathologically, and their physiological state was intact without pathological signs. In addition, we also evaluated the liver and kidney function of the healthy mice administered with the BUD, LNPs, and BUD-LNPs. In the serum analysis, blood samples were collected from the gastric artery of mice and analyzed 24 h after treatment. Importantly, after 3 days of intratracheal administration of BUD, LNPs, and BUD-LNPs, the levels of ALT, AST, AKP, BUN, CRE

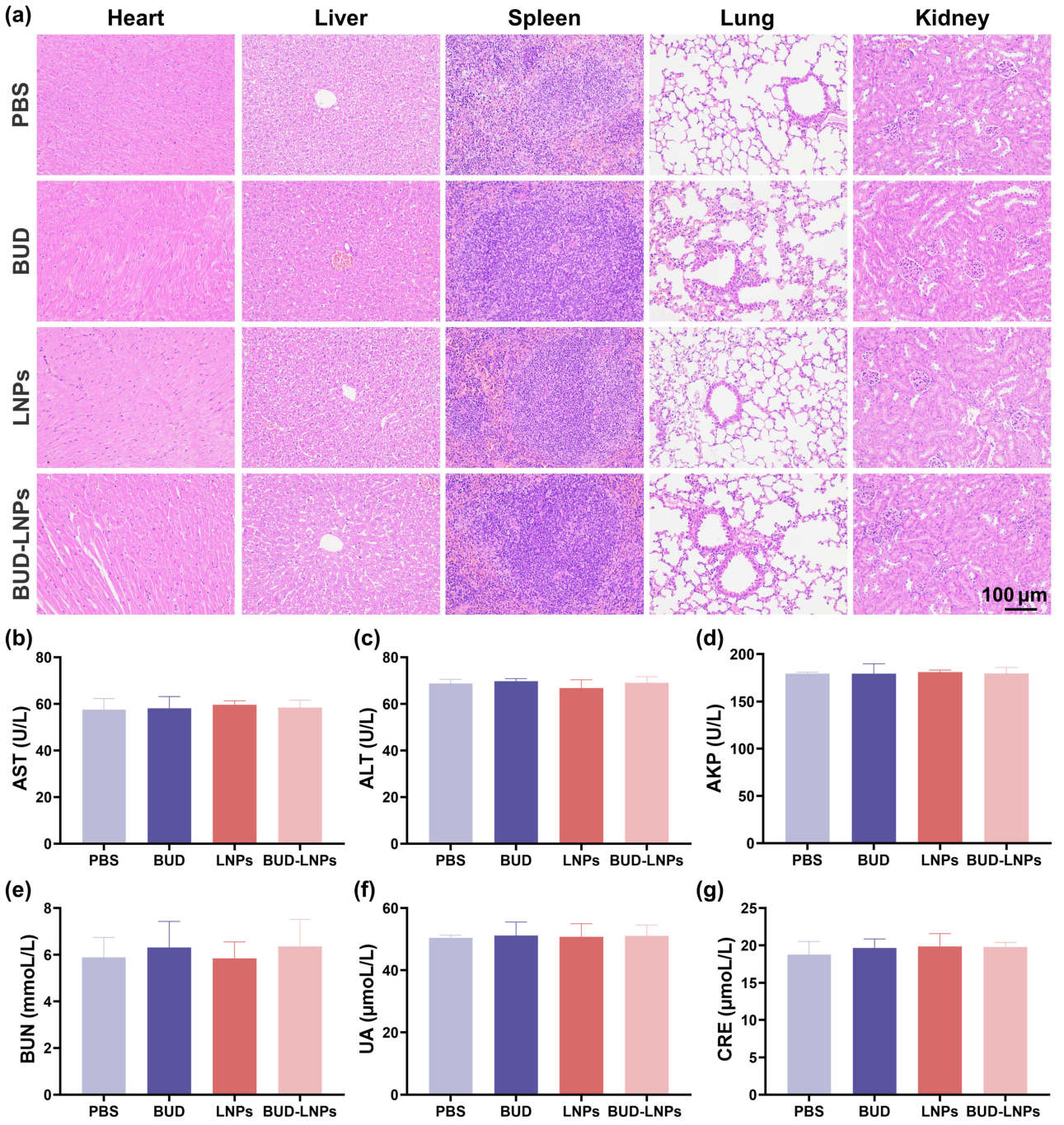

Figure 8 In vivo biocompatibility assessment of BUD, LNPs and BUD-LNPs. (**a**) H&E staining pictures of major organs of mice after intratracheal administration of BUD, LNPs and BUD-LNPs. Scale bar: 100 μm. Biochemical analysis results of (**b**) AST, (**c**) ALT, (**d**) AKP, (**e**) BUN, (**f**) UA and (**g**) CRE.

and UA showed no significant differences compared to the control group, indicating that intratracheal administration of BUD-LNPs (contained BUD 0.5 mg/kg) did not cause significant hepatotoxicity and nephrotoxicity (Figure 8b–g). The results demonstrated the use of pulmonary drug delivery device for topical administration may retain and localize BUD within a reservoir at the site of administration. In order to deliver sufficient doses of drugs to the lungs, liposomal nanomaterials, as the pulmonary drug delivery system, could increase the retention time of drugs in the lungs while reducing extrapulmonary side effects, resulting in improved therapeutic efficacy.[43] In conclusion, liposomal nanomaterials as the well-biocompatible, biodegradable, and nontoxic vesicles for encapsulating drugs, provided an attractive means for non-invasive drug delivery and sustained release in future asthma therapeutic drug development.[44]

Conclusion

In summary, we developed the BUD-LNPs for pulmonary drug delivery administration. Sustained release of BUD from liposomal nanoparticles was achieved in vitro with good biosafety and anti-inflammatory activity. Compared with the free drugs, the utilization of liposomal nano-vehicles for drugs delivery could effectively extend the duration of drugs accumulation in vivo. Furthermore, after delivery of BUD-LNPs to OVA-induced asthmatic mice, bronchial hyperresponsiveness was reduced, inflammatory factors in alveolar lavage fluid and the number of inflammatory cells in tissue sections were significantly reduced, and airway mucus secretion was also significantly reduced. And compared with other groups, BUD-LNPs showed superior therapeutic effect. BUD-LNPs showed good biocompatibility in vitro and in vivo, and were therapeutically effective in OVA-induced asthmatic mice. The integration of liposomal nano-vehicles into the design and development of novel pulmonary drug delivery systems holded the promise of significant clinical applications.

Acknowledgments

The authors are thankful to the Key Laboratory of Precision Infectious Diseases of Jilin Province (20200601011JC), Jilin Provincial Key Laboratory of Pathogen Biology International Science and Technology Cooperation (20230502002GH), the National Natural Science Foundation of China (52073278), the "Medical Science + X" Cross-innovation Team of the Norman Bethune Health Science of Jilin University (2022JBGS10), the Jilin Province Science and Technology Development Program (20230101045JC), the Education Department of Jilin Province (JJKH20231205KJ), then Health Commission of Jilin Province (2021JC036), and the Fundamental Research Funds for the Central Universities (2022-JCXK-09).

Disclosure

The authors report no conflicts of interest in this work.

References

1. Pavord ID, Beasley R, Agusti A, et al. After asthma: redefining airways diseases. *Lancet*. 2018;391(10118):350–400. doi:10.1016/s0140-6736(17)30879-6
2. Papi A, Brightling C, Pedersen SE, et al. Asthma. *Lancet*. 2018;391(10122):783–800. doi:10.1016/s0140-6736(17)33311-1
3. Ahmad A. Pharmacological strategies and recent advancement in nano-drug delivery for targeting asthma. *Life*. 2022;12(4):596. doi:10.3390/life12040596
4. Cevhertas L, Ogulur I, Maurer DJ, et al. Advances and recent developments in asthma in 2020. *Allergy*. 2020;75(12):3124–3146. doi:10.1111/all.14607
5. Bleecker ER, Menzies-Gow AN, Price DB, et al. Systematic literature review of systemic corticosteroid use for asthma management. *Am J Respir Crit Care Med*. 2020;201(3):276–293. doi:10.1164/rccm.201904-0903SO
6. Liang Z, Ni R, Zhou J, et al. Recent advances in controlled pulmonary drug delivery. *Drug Discov Today*. 2015;20(3):380–389. doi:10.1016/j.drudis.2014.09.020
7. Oh YJ, Lee J, Seo JY, et al. Preparation of budesonide-loaded porous PLGA microparticles and their therapeutic efficacy in a murine asthma model. *J Control Release*. 2011;150(1):56–62. doi:10.1016/j.jconrel.2010.11.001
8. Visaggi P, Barberio B, Del Corso G, et al. Comparison of drugs for active eosinophilic oesophagitis: systematic review and network meta-analysis. *Gut*. 2023;72(11):2019–2030. doi:10.1136/gutjnl-2023-329873
9. Pozzoli M, Rogueda P, Zhu B, et al. Dry powder nasal drug delivery: challenges, opportunities and a study of the commercial Teijin Puvlizer Rhinocort device and formulation. *Drug Dev Ind Pharm*. 2016;42(10):1660–1668. doi:10.3109/03639045.2016.1160110
10. Napp J, Markus MA, Heck JG, et al. Therapeutic fluorescent hybrid nanoparticles for traceable delivery of glucocorticoids to inflammatory sites. *Theranostics*. 2018;8(22):6367–6383. doi:10.7150/thno.28324
11. Zuo X, Guo X, Gu Y, et al. Recent advances in nanomaterials for asthma treatment. *Int J Mol Sci*. 2022;23(22). doi:10.3390/ijms232214427
12. Ortiz M, de Sa Coutinho D, Ciambarella BT, et al. Intranasal administration of budesonide-loaded nanocapsule microagglomerates as an innovative strategy for asthma treatment. *Drug Deliv Transl Res*. 2020;10(6):1700–1715. doi:10.1007/s13346-020-00813-5
13. Lokugamage MP, Vanover D, Beyersdorf J, et al. Optimization of lipid nanoparticles for the delivery of nebulized therapeutic mRNA to the lungs. *Nat Biomed Eng*. 2021;5(9):1059–1068. doi:10.1038/s41551-021-00786-x
14. Arber Raviv S, Alyan M, Egorov E, et al. Lung targeted liposomes for treating ARDS. *J Control Release*. 2022;346:421–433. doi:10.1016/j.jconrel.2022.03.028
15. Dymek M, Sikora E. Liposomes as biocompatible and smart delivery systems- the current state. *Adv Colloid Interface Sci*. 2022;309:102757. doi:10.1016/j.cis.2022.102757
16. Liu J, Wu Z, Liu Y, et al. ROS-responsive liposomes as an inhaled drug delivery nanoplatform for idiopathic pulmonary fibrosis treatment *via* Nrf2 signaling. *J Nanobiotechnology*. 2022;20(1):213. doi:10.1186/s12951-022-01435-4
17. Zhao J, Su J, Qin L, et al. Exploring the influence of inhaled liposome membrane fluidity on its interaction with pulmonary physiological barriers. *Biomater Sci*. 2020;8(23):6786–6797. doi:10.1039/d0bm01529f
18. Li H, Liu S, Dai W, et al. Pressure-sensitive multivesicular liposomes as a smart drug-delivery system for high-altitude pulmonary edema. *J Control Release*. 2023;365:301–316. doi:10.1016/j.jconrel.2023.11.039

19. Tang H, Chen J, Wang L, et al. Co-delivery of epirubicin and paclitaxel using an estrone-targeted PEGylated liposomal nanoparticle for breast cancer. *Int J Pharm*. 2020;573:118806. doi:10.1016/j.ijpharm.2019.118806
20. Wang J, Xu L, Liu X, et al. A facile adenosine triphosphate-responsive nanoplatform for efficacious therapy of esophageal cancer. *Oncol Lett*. 2020;20(4):108. doi:10.3892/ol.2020.11969
21. Guan X, Yuan Y, Wang G, et al. Ginsenoside Rg3 ameliorates acute exacerbation of COPD by suppressing neutrophil migration. *Int Immunopharmacol*. 2020;83:106449. doi:10.1016/j.intimp.2020.106449
22. Guan X, Lu Y, Wang G, et al. The role of regulatory T Cell in nontypeable Haemophilus influenzae-induced acute exacerbation of chronic obstructive pulmonary disease. *Mediators Inflamm*. 2018;2018:8387150. doi:10.1155/2018/8387150
23. Dunican EM, Elicker BM, Gierada DS, et al. Mucus plugs in patients with asthma linked to eosinophilia and airflow obstruction. *J Clin Invest*. 2018;128(3):997–1009. doi:10.1172/jci95693
24. Aegerter H, Lambrecht BN. The pathology of asthma: what is obstructing our view? *Annu Rev Pathol*. 2023;18:387–409. doi:10.1146/annurev-pathol-042220-015902
25. Chen D, Liu J, Wu J, et al. Enhancing nanoparticle penetration through airway mucus to improve drug delivery efficacy in the lung. *Expert Opin Drug Deliv*. 2021;18(5):595–606. doi:10.1080/17425247.2021.1854222
26. Schuster BS, Suk JS, Woodworth GF, et al. Nanoparticle diffusion in respiratory mucus from humans without lung disease. *Biomaterials*. 2013;34 (13):3439–3446. doi:10.1016/j.biomaterials.2013.01.064
27. Aalbers R, Vogelmeier C, Kuna P. Achieving asthma control with ICS/LABA: a review of strategies for asthma management and prevention. *Respir Med*. 2016;111:1–7. doi:10.1016/j.rmed.2015.11.002
28. Espinosa V, Rivera A. First line of defense: innate cell-mediated control of pulmonary aspergillosis. *Front Microbiol*. 2016;7:272. doi:10.3389/fmicb.2016.00272
29. Kuerban K, Gao X, Zhang H, et al. Doxorubicin-loaded bacterial outer-membrane vesicles exert enhanced anti-tumor efficacy in non-small-cell lung cancer. *Acta Pharm Sin B*. 2020;10(8):1534–1548. doi:10.1016/j.apsb.2020.02.002
30. Williams AH, Hebert AM, Boehm RC, et al. Bioscaffold stiffness mediates aerosolized nanoparticle uptake in lung epithelial cells. *ACS Appl Mater Interfaces*. 2021;13(43):50643–50656. doi:10.1021/acsami.1c09701
31. Wang Y, Wang X, Li Y, et al. Xuanfei Baidu Decoction reduces acute lung injury by regulating infiltration of neutrophils and macrophages *via* PD-1/IL17A pathway. *Pharmacol Res*. 2022;176:106083. doi:10.1016/j.phrs.2022.106083
32. Cao Y, Chen J, Ren G, et al. Punicalagin prevents inflammation in LPS-induced RAW264.7 macrophages by inhibiting FoxO3a/autophagy signaling pathway. *Nutrients*. 2019;11(11):2794.
33. Bianco A, Contoli M, Di Marco F, et al. As-needed anti-inflammatory reliever therapy for asthma management: evidence and practical considerations. *Clin Exp Allergy*. 2021;51(7):873–882. doi:10.1111/cea.13795
34. Almeida B, Nag OK, Rogers KE, et al. Recent progress in bioconjugation strategies for liposome-mediated drug delivery. *Molecules*. 2020;25(23). doi:10.3390/molecules25235672
35. Woodrow JS, Sheats MK, Cooper B, et al. Asthma: the use of animal models and their translational utility. *Cells*. 2023;12(7). doi:10.3390/cells12071091
36. Kim NY, Lee CH, Jin KN, et al. Clinical deterioration and lung function change in patients with concomitant asthma and bronchiectasis. *J Allergy Clin Immunol Pract*. 2022;10(10):2607–2613.e4. doi:10.1016/j.jaip.2022.05.026
37. Hayes D, Collins PB, Khosravi M, et al. Bronchoconstriction triggered by breathing hot humid air in patients with asthma: role of cholinergic reflex. *Am J Respir Crit Care Med*. 2012;185(11):1190–1196. doi:10.1164/rccm.201201-0088OC
38. Busse WW. The relationship of airway hyperresponsiveness and airway inflammation: airway hyperresponsiveness in asthma: its measurement and clinical significance. *Chest*. 2010;138(2 Suppl):4s–10s. doi:10.1378/chest.10-0100
39. Hochgerner M, Sturm EM, Schnoegl D, et al. Low oxygen levels decrease adaptive immune responses and ameliorate experimental asthma in mice. *Allergy*. 2022;77(3):870–882. doi:10.1111/all.15020
40. Hammad H, Lambrecht BN. The basic immunology of asthma. *Cell*. 2021;184(6):1469–1485. doi:10.1016/j.cell.2021.02.016
41. Athari SS. Targeting cell signaling in allergic asthma. *Signal Transduct Target Ther*. 2019;4:45. doi:10.1038/s41392-019-0079-0
42. Reddel HK, O'Byrne PM, FitzGerald JM, et al. Efficacy and safety of as-needed budesonide-formoterol in adolescents with mild asthma. *J Allergy Clin Immunol Pract*. 2021;9(8):3069–3077.e6. doi:10.1016/j.jaip.2021.04.016
43. Chipps BE, Israel E, Beasley R, et al. Albuterol-budesonide pressurized metered dose inhaler in patients with mild-to-moderate asthma: results of the DENALI double-blind randomized controlled trial. *Chest*. 2023;164(3):585–595. doi:10.1016/j.chest.2023.03.035
44. Bassetti M, Vena A, Russo A, et al. Inhaled liposomal antimicrobial delivery in lung infections. *Drugs*. 2020;80(13):1309–1318. doi:10.1007/s40265-020-01359-z